Al-Sibd Center for Research and Scholarly Publishing

Journal of Energy Sustainability and Economics (JESE)

Journal Homepage : https://jese.srp-center.iq/

New Approach For Decline Curve Analysis of Unconventional Fractured Reservoirs: Rate-Normalized Flow Rate Derivative Concept

Salam Al-Rbeawi[1] ،Fadhil S. Kadhim[2], Jalal Owayed[3]

[1]University of Warith Al-Anbiyaa, Iraq, [2]University of Technology, Iraq, [3]Kuwait University, Kuwait

Corresponding Author : salam.jabar@uowa.edu.iq

Keywords:

Decline curve analysis;
Unconventional resources;
Fractured reservoirs;
Production forecasting;
Reserve estimation

Abstract

This manuscript introduces a new decline curve analysis (DCA) technique to analyze and predict the potentials of hydraulically fractured unconventional resources. The new approach relies on the rate-normalized flow rate derivative (RNFD) concept. It uses the significant constant behavior of the RNFD that identifies the power-law type flow regime models of fractured reservoirs. This technique merges the RNFD with a new numerical model for the flow rate derivative (flow rate noise-reducing derivative model).

The concept of the RNFD [1/q (txq^')] is developed based on the power-law type analytical models of the flow regimes that can be characterized from the production history of gas or oil-producing wells. The production rate, cumulative production, and the calculated RNFDs from the production history are used for this purpose. The constant RNFD values and the flow rate derivative's numerical model can be used to simulate the production history or predict future performance. The impact of the skin factor is introduced to the approach by developing new RNFD models that could replace the constant pattern of RNFD when this impact does not exist. For a severe condition of skin factor, the RNFD shows a linear relationship with time instead of the constant value. The proposed approach gives an excellent match with the production history of the case studies examined in this study. The transition between flow regimes does not impact the application of the RNFD, i.e., the calculations move very smoothly throughout the flow regime.

The novelty of the proposed technique is represented by introducing an approach for the DCA that considers the observed flow regimes during the production history and the impact of the skin factor. The approach proposes new numerical flow rate and cumulative production models to predict future performance as well as new models for estimating the impact of skin factors on production history, especially for early time flow regimes.

Introduction

Unconventional shale reservoirs are characterized by a complex structure with high heterogeneity, anisotropy, and very low permeability that could be in the range of a few nano-Darcies. The pressure changes caused by the production from these reservoirs move very slowly in the reservoir, and the reservoir boundaries may need a long time to be reached and pseudo-steady state flow to be observed. The common practice for developing these reservoirs is hydraulic fracturing stimulation, where thin and long fractures are created in the drainage area. The permeability of these fractures may reach thousands of milli-Darcies, and the permeability of the reservoir matrix called stimulated reservoir volume (SRV), might be enhanced significantly due to the induced microfractures. The primary hydraulic fractures and the induced microfractures offer open channels for reservoir fluid transportation from the matrix toward the wellbores.

Pressure and rate transient analysis are two characterization tools commonly applied to conventional and unconventional oil and gas reservoirs. The DCA is widely used for predicting the future performance of these reservoirs. It attempts to find a model that fits the production history and is confidently utilized to predict future performance. The concept depends on the fact that the previous production pattern and the controlling parameters may dominate future production with no changes. The most used models of decline curve behavior were developed by Arps in 1944 and used for forecasting the future potential of oil reservoirs (Arps 1945). These models were created by the nonlinear regression analysis of the produced oil or gas based on the assumptions that the production at any time is a constant decline fraction of the initial production, i.e., the concept presented by Johnson and Bollens 1927 of the loss ratio for the decline curves. Arps has presented three equations emphasizing that the hyperbolic decline is the most commonly seen. The harmonic decline is not seen frequently, while the exponential decline is simple but less accurate. The traditional Arps' equations have not considered the properties of reservoir rock and fluids, and the wellbore type and reservoir configurations. Moreover, the impact of the flow regimes that developed during the entire production time has not been considered.

More than three decades later, Fetkovich stated that the Arps approach is suitable only for the late time when the boundary-dominated flow (BDF) regime is reached (Fetkovich 1980; Fetkovich et al. 1987; Fraim and Wattenbarger 1987; Fetkovich et al. 1996). Fetkovich confirmed that the three models give misleading results if the production data sets do not belong to the BDF conditions. He introduced some wellbore and reservoir parameters to the decline curve models and presented the well-known type curve approach. Blasingame and Rushing (2005) reached the same conclusion, illustrating that the Arps' relations may lead to unrealistic results and extrapolations. They proposed a quadratic model to calculate dry gas reservoirs' anticipated rate and cumulative production. This model couples the stabilized flow equation of a constant bottom-hole pressure condition and the production time calculated based on the material balance concept. Before that, the material balance time was used by Blasingame and Lee 1986 and included in the DCA models to interpret the variable-rate data of the late production time. While Fraim and Wattenbarger 1987 introduced the pseudo-time concept to reduce the non-linear behavior from these models. Hsieh et al. 2001 argued that the Arps' equations do not consider the variability of the petrophysical properties, such as the permeability due to the reservoir conditions. The primary concern of Lee and Sidle 2010 was the unreasonable physical properties that control the production may narrow the applicability of the conventional DCA models. These concerns are raised when the value of the constant ($b > 1.0$), although the best fit of the hyperbolic decline is

seen with the long transient production data of shale and tight reservoirs. While the major concern of Luo et al. 2014 was the uncertainties that govern the production forecasting of the traditional DCA. Thus, the rate transient analysis might help justify the DCA assumptions and eliminate the uncertainties.

It can be said that Arps' decline curves are not recommended for the reservoirs where the transient state conditions could dominate the flow for a long time. These curves could work perfectly at late production time after reaching the BDF, similar to the flow conditions in the porous media of unconventional shale reservoirs. Therefore, several researchers have adopted and presented new models during the last few decades to interpret unconventional plays' production behavior. Stright and Gordon 1983 suggested using the production records of one or two years to foresee the reservoir performance characterized by low permeability by a decline curve model that only represents a linear flow. The concept of utilizing linear flow characteristics in hydraulically fractured reservoirs was adopted later by El-Banbi and Wattenbarger 1998 and Wattenbarger et al. 1998. Their argument for this adaptation relied on the consumed time by the linear flow regime that may reach 10-20 years in extra low permeability reservoirs. In reality, developing a decline curve model based on the analytical model of linear flow regime is a relatively easy task.

Several parameters may impact the production data analysis of unconventional plays rather than the flow conditions only. These parameters are the degree of geological complexities, the existence of natural fractures, the flow mechanisms inside the matrix and fluid flux through the matrix-fracture interface. Because of that, the decline curve models would be more challenging (Ilk et al. 2010; Gupta et al. 2018). These challenges motivated the development of new DCA models, such as the empirical "power-law exponential rate"10 adopted by Mattar et al. 2008 for complex wells. In their study, two approaches were presented, one is simple, and the other is more rigorous, wherein they verified the "compound linear flow regime" presented by van Kruysdijk and Dullaert 1989. The compound linear flow refers to the bi-linear flow (BLF) wherein reservoir fluids in the matrix flow to the fractures first and, after that, to the wellbores. It is typically observed after early hydraulic fracture linear flow (HFLF) regime when an individual fracture has interfered with other nearby fractures due to its bad conductivity (Ilk et al. 2011). While Valko 2009, and Valko and Lee 2010 claimed using a specialized DCA methodology, called stretched exponential production decline SEPD, for more than 7000 production histories taken from the Barnet shale reservoirs in the USA. According to Valko, the methodology helped detect the significant changes in production behavior and calculate the jumps in the ultimate recovery. The "logistic growth model LGM" was used by Clark et al. 2011 for forecasting extralow permeability resources. In this model, the knowing physical volumetric quantities are incorporated into the LGM model to increase the accuracy of the reserve estimation. Egbe et al. 2023 combined two Bayesian methods and two frequentist methods with five DCA techniques: Arps, Duong, SEPED, power-law, and LGM for analyzing more than 1,800 historical production data sets.

With no consideration given to the traditional decline curve models, Bello and Wattenbarger 2010 comprehensively reviewed the linear and BLF regimes of multistage hydraulically fractured reservoirs. While Minin et al. 2011 suggested a methodology for reserve estimation in unconventional plays using the decline curve models that follow a probabilistic approach. Similarly, Can and Kabir 2012 recommended a workflow for the reserve evaluation that couples a stretched-exponential production decline (SEPD) with a probabilistic forecasting frame. The dilemma of constant bottom-hole pressure

required by traditional decline curve models was studied by Ayala and Zhang 2013. They rescaled and extended the exponential and density-based decline curve models to be applied to the variable rate and pressure conditions. They confirmed that their proposed models are able to analyze the changes in the rate-pressure downhole conditions, such as the step-changes in the pressure and sandface flow rate. While Sureshjani and Gerami 2011 introduced a decline curve model for two-phase flow conditions that is used to anticipate the performance of condensate reservoirs. They converted the exponential decline to a harmonic decline using a time function to consider the continuous changes in the operating conditions.

A new approach for predicting the foreseen rate and the EUR of hydraulically fractured reservoirs was presented by Duong 2011. This approach provides a statistical protocol to analyze the production records of unconventional resources and formulate a range of parameters for the forecasting process. Shahamat et al. 2015 presented the skin factor impact on the DCA by merging a function called Beta-Derivative to the characteristics of linear and BDF regimes. They stated that this function could demonstrate a constant value with time (0.5) for linear flow and a straight line of a unit slope for the BDF. The idea of Beta-Derivative was introduced by Ilk et al. 2007 and used in the DCA by Idorenyin et al. 2011. This function is a constant for the linear, bi-linear, and BDF regimes. Idorenyin et al. 2011 connected the Beta-Derivative with the analytical solution of the BDF regime.

The impacts of the matrix permeability of hydraulically fractured reservoirs, unstimulated reservoir volume, primary fractures and induced microfractures network, and gas adsorption mechanisms on the production decline trend have been studied by Wang 2016. de Holanda et al. 2018 combined different aspects, including physical and statistical information, to the DCA of unconventional resources. Xi and Morgan 2019 combined the DCA and geostatistical features to predict the production of Marcellus shale gas plays in the USA. They used the production data of wells with more than 24 months of history to ensure good decline behaviors. Maraggi et al. 2023 claimed developing a new approach to apply DCA for tight reservoir under variable bottom hole flowing pressure. In this approach the DCA parameters, bottom hole flowing pressure, and the initial reservoir pressure are predicted using the superposition theory and the constant-pressure solution of the diffusivity equation.

The transportation of reservoir fluids in the matrix of unconventional reservoirs is more complex to be described by the viscous flow (Raghavan and Chen 2017). The high level of heterogeneity causes an increase in the degree of complexity in these reservoirs (Liu and Emami-Meybodi, 2021). Therefore, the traditional decline curves may not fit the actual production data during transient or boundary-dominate flow conditions. Liu and Valko 2019 developed a DCA model to consider the anomalous diffusive flow in the structurally complex porous media. They claimed to obtain a good match between the results of their model and the real data of multiple-fractured horizontal wells in the Permian Basin, USA. Hazlett et al. 2021 introduced a discrete fracture model that incorporates the traditional decline curve models to predict the performance of fractured reservoirs considering different reservoir configurations, fracture geometries, and matrix permeability. While Chavali and Lee 2021 assembled the probabilistic distribution with the DCA models to predict oil production using Monte Carlo simulation. He et al. 2022 considered a case study of Jimsar shale oil in the Northwest China to apply the DCA. They combined the production data, and well and reservoir data to the Arps equation, Duong model, flow material balance method, and the Blasingame type-curve to predict the future performance and the ultimate recovery.

Digital applications have recently been utilized in all disciplines, not just the petroleum industry. Machine learning is a digital tool that uses large data sets to predict a specific trend or behavior. The process requires several steps starting with collecting, classifying, and analyzing the data. Part of the available data is used to build the best-fit model examined by the remaining data. Finally, the machine-learning model is applied to predict future performance. The production history offers the data sets that machine learning algorithms require. Fulford et al. 2016 stated that machine learning is an excellent tool for interpreting unconventional resources' time/rate patterns. They suggested that the probabilistic DCA and Markov-chain Monte Carlo simulation can be used to evaluate the reserves uncertainty numerically. Alarifi and Miskimins 2021 introduced an approach for the ultimate recovery (EUR) of hydraulically fractured reservoirs using machine learning algorithms. This approach utilizes the production history and decline curve characteristics to develop a predictive model for EUR estimation using an artificial neural network. While Liu et al. 2021 used the "gray-box" approach that incorporates the strength of physics-based models into machine learning-developed models for developing a tool to forecast the potentials of unconventional reservoirs. A simplified workflow called dynamic production rescaling was created by Li et al. 2021 to increase the accuracy of DCA by the machine.

This paper introduces a new decline curve technique to predict the future performance of unconventional hydraulically fractured reservoirs. This technique depends on the concept of the RNFD that demonstrates a constant behavior for all flow regimes. The paper also introduces a numerical solution for the flow rate derivative adjusted for calculating future flow rates. According to the observed flow regimes from the production history, the RNFD and the numerical solution of the flow rate derivative are gathered to simulate the flow rate. At the same time, the RNFD of the last seen flow regime is used to forecast the performance with the aid of the numerical solution of the flow rate derivative. The motivation of this study is to introduce a DCA technique that is easily applied with no limitations and considerations given to the wellbore and reservoir conditions. The proposed approach is a promising forecasting tool that could eliminate the impacts of the uncertainties and misleading behaviors raised by the unique characteristics of unconventional reservoirs, such as extra low permeability and complex structures.

Analytical models

The Duhamel principle can mathematically formulate the analytical model of the sandface flow rate of an unconventional reservoir depleted by a horizontal wellbore intersecting multiple hydraulic fractures, assuming constant bottom hole flowing pressure (van Everdingen 1949).

$$\bar{q}_D = \mathcal{L}^{-1}\left(\frac{1}{s^2\bar{P}_{wD}}\right) \quad (1)$$

while the analytical model of cumulative production is given by (Helmy and Wattenbarger 1998):

$$\bar{N}_{PD} = \int_0^{t_D} \bar{q}_D \, d\tau_D = \frac{1}{s^3\bar{P}_{wD}} \quad (2)$$

Eqs. (1) and (2) include the pressure term ($\bar{P}_{wD}$). ($\bar{P}_{wD}$) is the pressure drop of a horizontal wellbore intersecting multiple hydraulic fractures when the sandface flow rate is assumed constant. This pressure term is calculated by (Brown et al. 2011, Ozkan, O. et al. 2014; Al-Rbeawi 2018):

$$\bar{P}_{wD} = \frac{\pi}{sF_{CD}\sqrt{A_F}tanh\left(\sqrt{A_F}\right)} \quad (3)$$

Eq. (3) is applied for a rectangular drainage area (x_{eD}, y_{eD}) with stimulated and unstimulated reservoir volumes, as shown in Fig. (1). Stimulated reservoir volume (SRV) is the pours media where the hydraulic fractures are propagated. In contrast, these fractures do not exist in the unstimulated reservoir volume (USRV). Eq. (3) is developed for symmetrically distributed hydraulic fractures with equal fracture half-length (x_f) and fully penetrating the reservoir in the vertical direction, i.e., fracture height equals formation thickness (h). Natural fractures are assumed to be arbitrarily distributed in the matrix of SRV and USRV.

The term (A_F) in Eq. (3) represents the reservoir configurations and the characteristics of the SRV and USRV. It is given by:

$$A_F = \frac{2B_F}{F_{CD}} + \frac{s}{\eta_{fD}} \quad (4)$$

where:

$$B_F = \sqrt{A_r}\tanh\left[\sqrt{A_r}(y_{eD} - w_D/2)\right] \quad (5)$$

$$A_r = \frac{B_r}{R_{CD}y_{eD}} + sf(s) \quad (6)$$

$$B_r = \sqrt{\frac{s}{\eta_{rD}}}\tanh\left[\sqrt{\frac{s}{\eta_{rD}}}(x_{eD} - 1)\right] \quad (7)$$

The dimensionless conductivity (F_{CD}) in Eqs. (3), and (4) depends on the fracture width (w_f) and half-length (x_f) as well as fracture and SRV matrix permeabilities:

$$F_{CD} = \frac{k_f w_f}{k_{srv} x_f} \quad (8)$$

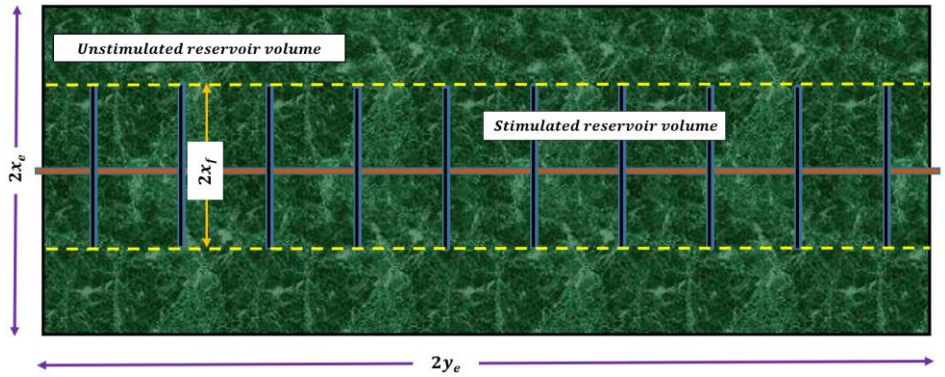

Figure 1: Rectangular unconventional reservoir depleted by multiple hydraulic fractures.

The typical flow rate and cumulative production behavior of hydraulically fractured reservoirs are calculated using Eqs. (1) and (2), respectively, are shown in Figs. (2), and (3). These two figures represent the impacts of different hydraulic

fracture conductivities and reservoir drainage areas on the flow rate and cumulative production. The comments that can be inferred from Figs. (2) and (3) are:

1- Non-Linear behavior significantly dominates the flow rate and cumulative production relationships with production time. Therefore, it is difficult to model and forecast future performance using the traditional decline curve models. The non-linear behavior is due to the development of different flow regimes during the production and the exitance of various porous media in the fractured reservoirs. These porous media have different petrophysical properties. The hydraulic fractures are considered porous media of high porosity-permeability, while the USRV is characterized by ultralow permeability. The fracturing process enhances the permeability of the SRV but still much less than the permeability of hydraulic fractures. The non-linearity could become sharper, knowing that most unconventional reservoirs may have complex structures and the flow mechanisms are closer to the diffusion flow than Darcy (viscous flow) or non-Darcy flow (Al-Rbeawi 2020).

2- Four flow regimes can be identified from the production life of unconventional reservoirs. The (HFLF) regime is the first. This regime represents the linear flow of reservoir fluids inside these fractures and is defined by a slope of (1/2) on the log-log plot of the flow rate and production time. The second is the BLF regime prescribed by a slope of (0.25) on the same plot. It is the simultaneous linear flow of reservoir fluid from the SRV to the fractures and, after that, to the wellbore. The flow from unstimulated to stimulated reservoir volume is represented by the third flow regime, i.e., the formation linear flow (FLF) regime defined by a slope of (0.5). The abovementioned three flow regimes are developed during early and late transient flow conditions that may last for a long time, i.e., the whole production life of unconventional reservoirs. The fourth flow regime might not be seen as it represents the BDF when the impact of the reservoir boundary has occurred. This flow regime is defined by a slope of (1.0) on the log-log plot of the flow rate and production time.

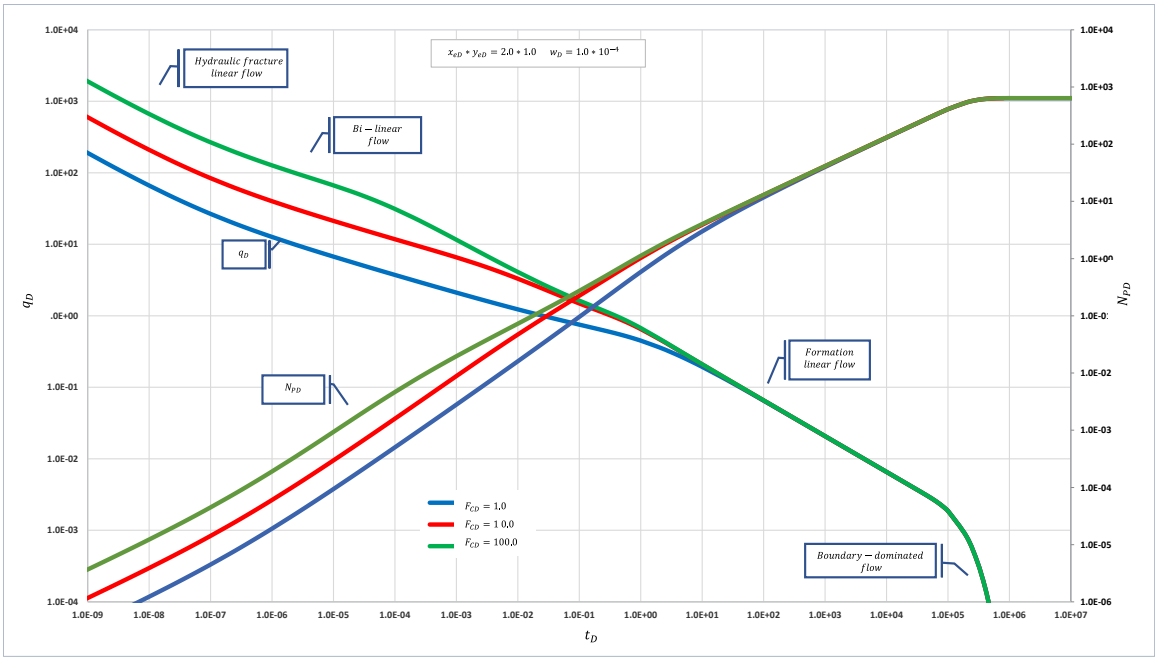

Figure 2 : Flow rate and cumulative production behavior for different hydraulic fracture conductivities.

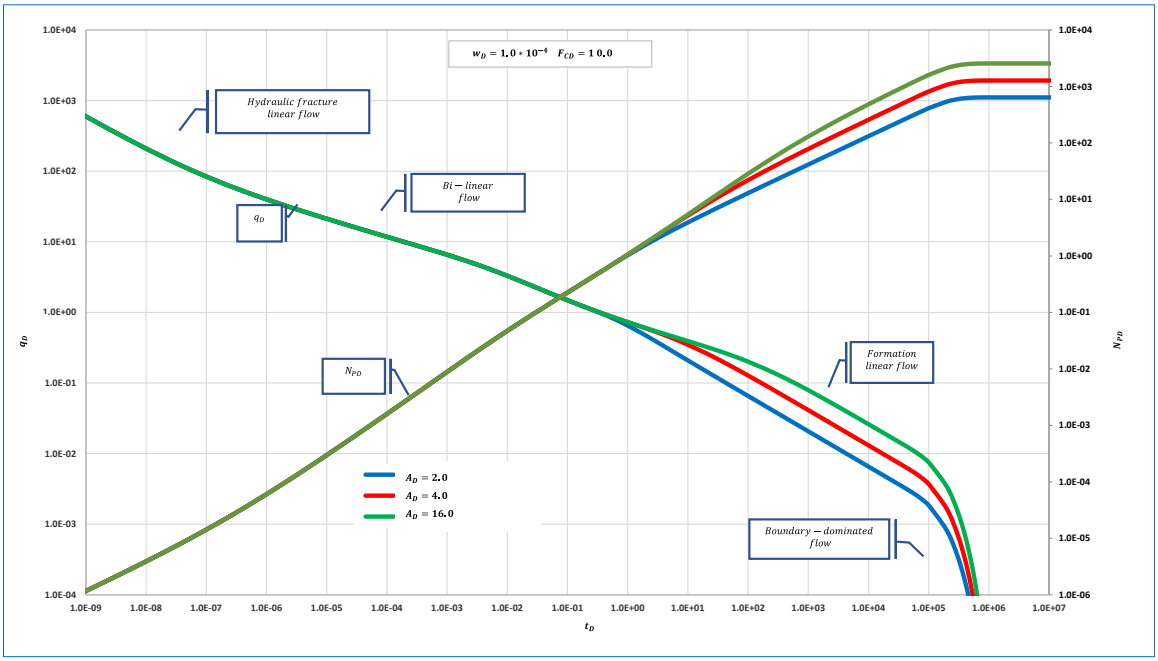

Figure 3: Flow rate and cumulative production behavior for different drainage areas.

Eq. (1) can be solved for the HFLF regime where the fracture conductivity is the controlling parameter. The analytical model of the flow rate, in dimensionless form, for this flow regime is given by (Bello et al. 2010; Kuchuk et al. 2016):

$$q_D = Ct_D^{-1/2} \quad (9)$$

where (C) is a constant that depends mainly on the dimensionless conductivity. While the cumulative production during this flow regime is given by:

$$N_{PD} = \int_0^{t_D} q_D d\tau_D = 2\,C t_D^{1/2} \quad (10)$$

The flow rate analytical model of the BLF regime is derived from the solution of Eq. (1), considering the petrophysical properties of the SRV and the fracture half-length. This model, in dimensionless form, is given by:

$$q_D = C t_D^{-1/4} \quad (11)$$

where (C) is a constant that depends on the dimensionless conductivity and the characteristics of the SRV. While the cumulative production during this regime is:

$$N_{PD} = \int_0^{t_D} q_D d\tau_D = \frac{4}{3} C t_D^{3/4} \quad (12)$$

The flow rate analytical model of the FLF regime is obtained from the solution of Eq. (1), considering the petrophysical properties of SRV and USRV and the spacing between hydraulic fractures. This model, in dimensionless form, is given by:

$$q_D = C t_D^{-1/2} \quad (13)$$

where (C) is a constant that depends on the petrophysical properties of SRV and USRV and the spacing between hydraulic fractures. While the cumulative production during this flow regime is:

$$N_{PD} = \int_0^{t_D} q_D d\tau_D = 2\,C t_D^{1/2} \quad (14)$$

The distance to the reservoir boundaries controls the BDF regime. Therefore, the flow rate model during this flow regime can be approximated from Eq. (1) to:

$$q_D = \frac{a}{2\pi x_{eD} y_{eD}} t_D^{-1} + b \quad (15)$$

where (a) and (b) are two constants. While the cumulative production during the BDF regime is:

$$N_{PD} = \int_0^{t_D} q_D d\tau_D = \frac{a}{2\pi x_{eD} y_{eD}} ln(t_D) + b t_D \quad (16)$$

The production rate and cumulative production models, given in Eqs. (9), (10), (11), (12), (13), (14), (15), and (16) can be converted to real-time parameters using the mathematical formulations of the dimensionless parameters presented in Appendix-A. However, the real-time models are difficult to be used to predict the reservoirs' future performance as they contain many petrophysical parameters, hydraulic fracture dimensions, and reservoir boundaries.

Rate-normalized flow rate derivative (RNFD)

In this study, the RNFD technique is developed to eliminate the non-linear behavior of the production rate with the production time. The objective of the RNFD is to change the non-linear behavior to a linear behavior that can be employed to forecast future performance. Mathematically, the RNFD is defined, in dimensionless and real-time parameters, by:

$$RNFD = \frac{1}{q_D}(t_D x q'_D) = \frac{1}{q}(t x q') \quad (17)$$

where:

$$(t_D x q'_D) = \frac{(q_{Di} - q_{Di-1}) \frac{[ln(t_{Di+1}) - ln(t_{Di})]}{[ln(t_{Di}) - ln(t_{Di-1})]} + (q_{Di+1} - q_{Di}) \frac{[ln(t_{Di}) - ln(t_{Di-1})]}{[ln(t_{Di+1}) - ln(t_{Di})]}}{[ln(t_{Di+1}) - ln(t_{Di-1})]} \quad (18)$$

Analytically, the RNFD of the HFLF regime is derived from Eq. (9) as follows:

$$\frac{1}{q_D}\left(t_D x q_D^{'}\right) = \frac{1}{q}\left(t x q^{'}\right) = -\frac{1}{2} \quad (19)$$

while the RNFD of the BLF regime is obtained from Eq. (11):

$$\frac{1}{q_D}\left(t_D x q_D^{'}\right) = \frac{1}{q}\left(t x q^{'}\right) = -\frac{1}{4} \quad (20)$$

Similarly, the RNFD of the FLF regime is derived from Eq. (13):

$$\frac{1}{q_D}\left(t_D x q_D^{'}\right) = \frac{1}{q}\left(t x q^{'}\right) = -\frac{1}{2} \quad (21)$$

and the RNFD of the BDF regime is obtained from Eq. (15):

$$\frac{1}{q_D}\left(t_D x q_D^{'}\right) = \frac{1}{q}\left(t x q^{'}\right) = -1 \quad (22)$$

Eqs. (19), (20), (21), and (22) state that the RNFD behavior of the four flow regimes demonstrates a constant value with production time. Four horizontal lines appear when the RNFD is plotted vs production time. This fact can be proved by utilizing the calculated flow rates from Eq. (1), presented in Figs. (2), and (3) to calculate the RNFD of the production life of the reservoirs. For this purpose, a numerical solution, in dimensionless form, for the flow rate derivative is proposed in this study. This model calculates the flow rate derivative using three production times and the corresponding flow rates:

$$\frac{1}{q_D}\left(t_D x q_D^{'}\right) = \frac{\left[\frac{(q_{Di}-q_{Di-1})}{q_{Di}}\right]\frac{[ln(t_{Di+1})-ln(t_{Di})]}{[ln(t_{Di})-ln(t_{Di-1})]}+\left[\frac{(q_{Di+1}-q_{Di})}{q_{Di}}\right]\frac{[ln(t_{Di})-ln(t_{Di-1})]}{[ln(t_{Di+1})-ln(t_{Di})]}}{[ln(t_{Di+1})-ln(t_{Di-1})]} \quad (23)$$

Eq. (23) gives the RNFD in dimensionless parameters; however, the RNFD in real-time parameters is similar, except $(q_D, t_D, and\ q_D')$ are replaced by $(q, t, and\ q')$. The calculated RNFD is plotted vs. production time on the log-log plot, as shown in Figs. (4), and (5). These two figures tell us the followings:

1- The RNFD has the same behavior regardless of the reservoir configuration, petrophysical properties of the SRV and USRV, and hydraulic fracture dimensions and conductivity.
2- Four horizontal lines are observed with production time. Each horizontal line represents a flow regime and has a constant RNFD along the time elapsed by this flow regime. Sometimes the HFLF regime might not be observed when it lasts for a short time in cases where these fractures have good conductivity. The BDF regime also might not be seen as the transient state conditions could dominate the porous media of unconventional reservoir for a long time, and the reservoir boundary impact might not be felt, i.e., pseudo-steady state conditions have never been reached.

The linear behavior of the RNFD of the four flow regimes supports the approach presented in this study for applying the RNFD to predict future performance and simulate the production history. In this study, the assembly of the constant value of the RNFD of the four flow regimes, given in Eqs. (19-22) and the real-time parameters of Eq. (23) are suggested to be used for the flow rate forecasting as follows:

$$q_{i+1} = \left\{q_i(\beta RNFD)[ln(t_{i+1}) - ln(t_{i-1})] - (q_i - q_{i-1})\frac{[ln(t_{i+1})-ln(t_i)]}{[ln(t_i)-ln(t_{i-1})]} + q_i\frac{[ln(t_i)-ln(t_{i-1})]}{[ln(t_{i+1})-ln(t_i)]}\right\}\frac{[ln(t_{i+1})-ln(t_i)]}{[ln(t_i)-ln(t_{i-1})]} \quad (24)$$

Eq. (24) makes forecasting flow rate very easy, wherein only (β) and the RNFD are required to be determined for each flow regime. To predict the flow rate (q_{i+1}) at any time step in the future (t_{i+1}), the last two flow rates (q_i) and (q_{i-1}) of the

production history and the corresponding two production times (t_i) and (t_{i-1}) are required. The true flow rate at any time step is calculated by averaging three flow rates as follows:

$$q = \frac{q_{i+1}+q_i+q_{i-1}}{3} \quad (25)$$

The cumulative production can be predicted by:

$$N_P = \sum_1^N (t_{i+1} - t_i)\left\{q_i(\beta RNFD)[ln(t_{i+1}) - ln(t_{i-1})] - (q_i - q_{i-1})\frac{[ln(t_{i+1})-ln(t_i)]}{[ln(t_i)-ln(t_{i-1})]} + q_i\frac{[ln(t_i)-ln(t_{i-1})]}{[ln(t_{i+1})-ln(t_i)]}\right\}\frac{[ln(t_{i+1})-ln(t_i)]}{[ln(t_i)-ln(t_{i-1})]} \quad (26)$$

The (EUR) can be determined either graphically from the semi-log plot of the cumulative production or analytically from the cumulative production, calculated by Eq. (26), after 20 years, for example, such that:

$$EUR|_{20years} = N_P|_{20years} \quad (27)$$

The correction factor (β), shown in Eqs. (24) and (26) depends on the slope of the straight lines of the flow regimes observed on the log-log plot of the flow rate and the production time. The correction factor of FLF, for example, is $(\beta = 3.0)$. It is calculated from the slope of the FLF regime (1/2) and the slope of the BLF regime (1/4), as shown in Fig. (6a). While it is (1.5) for the BDF as it is depicted from Fig. (6b).

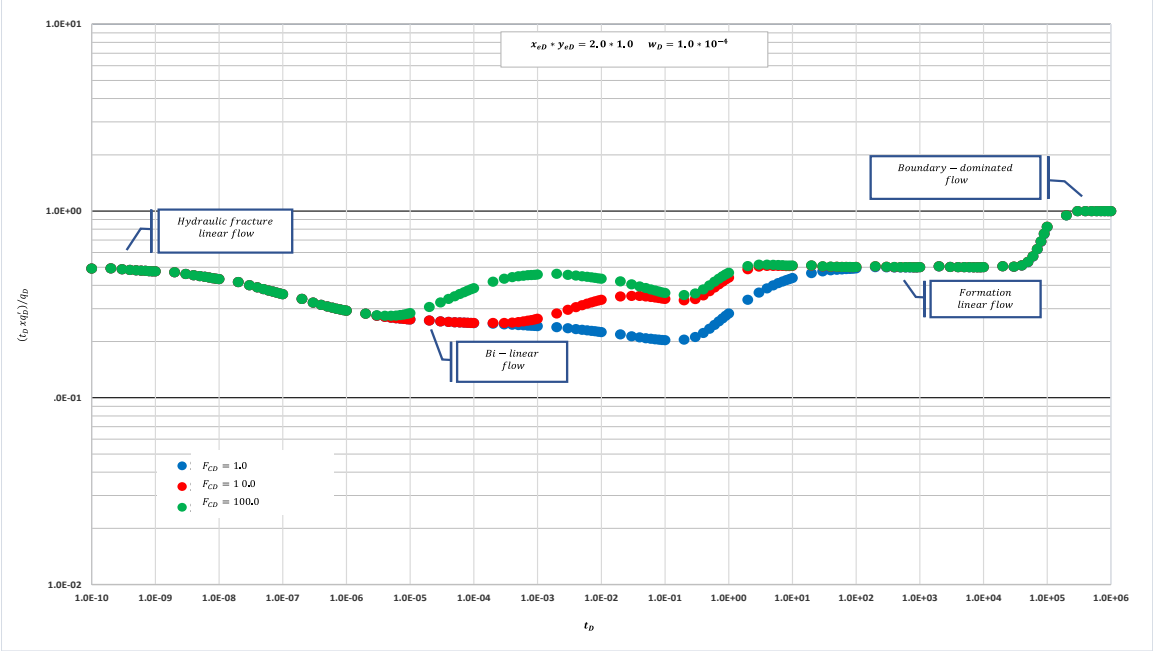

Figure 4: RNFD behavior of different hydraulic fracture conductivities.

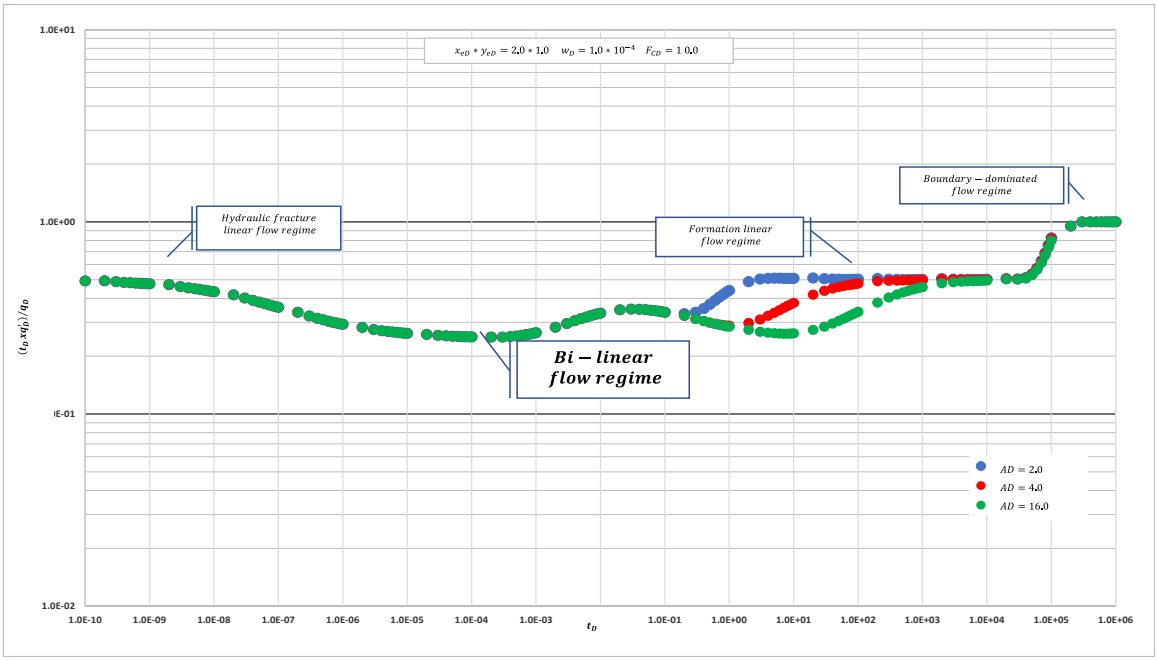

Figure 5: RNFD behavior of different drainage areas.

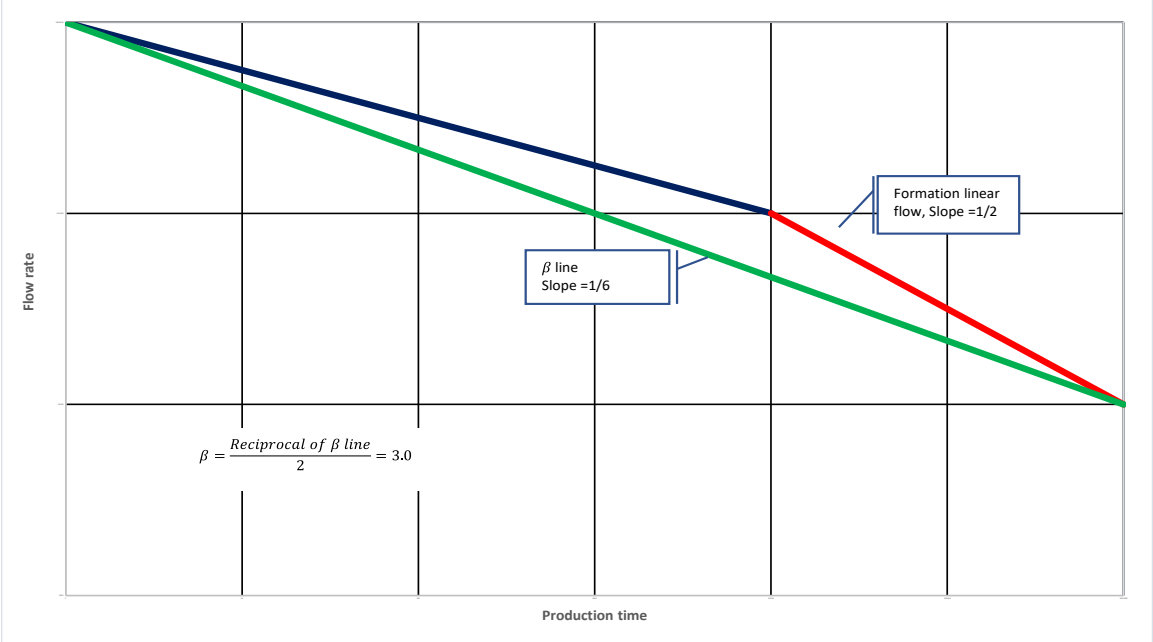

Figure 6: (a) Correction factor calculation- FLF regime.

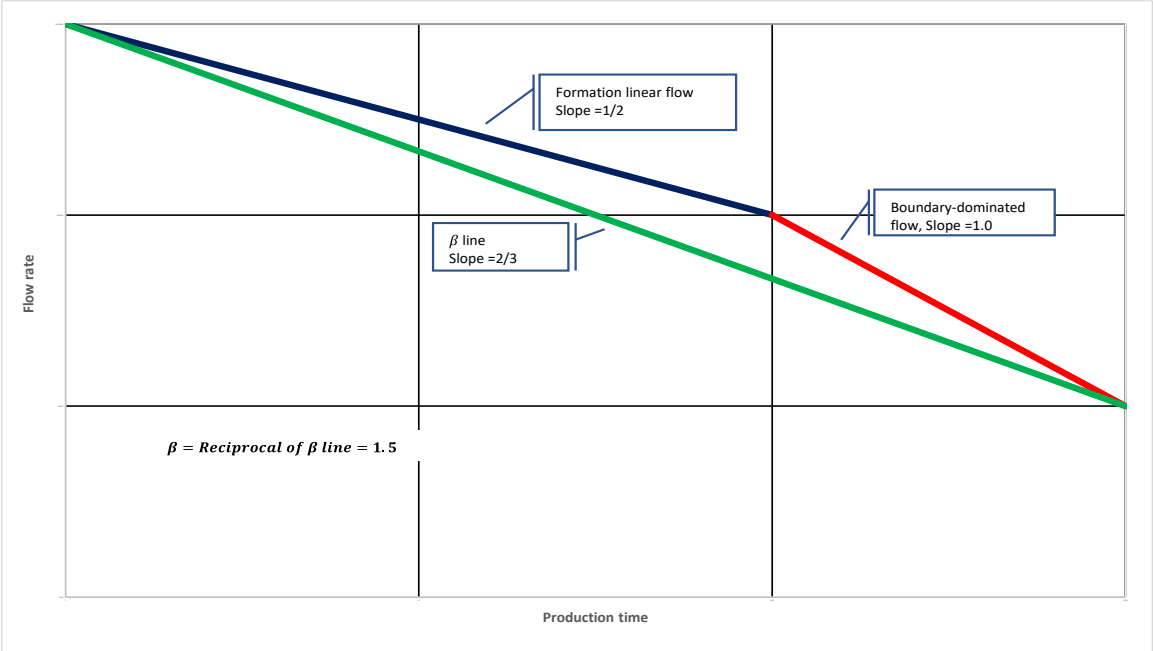

Figure 6: (b) Correction factor calculation- BDF regime.

The sequential steps required for applying the RNFD approach as a decline curve technique are:

1- From the production history of a producing well, plot the production rate (q) vs. production time on the log-log scale. Characterize the dominant flow regimes from the slope of the flow rate curve wherein the hydraulic fracture and FLF regimes demonstrate a straight line of a slope (-0.5). The BLF regime appears as a straight line of slope (-0.25), while the BDF regime shows a unit slope line (-1).

2- Estimate each observed flow regime's starting and ending time from the log-log plot of the production rate vs. time. The intersection points between the flow regime lines could be used for this purpose.

3- Calculate the RNFD for each production time using Eq. (23) and plot the RNFD vs production time. Check the observed flow regimes and the horizontal lines of a constant RNFD.

4- Using the first two flow rates and the corresponding production times at the beginning of the first flow regime observed at early production time and the calculated RNFD, calculate the third flow rate using Eq. (24). Continue the flow rate calculations until the last flow rate of the first flow regime.

5- Calculate the correction factor (β) required for the second flow regime. The correction factor is necessary to correct the slope of the flow regimes. It is (3.0) when the calculation of the flow rate during HFLF regime reaches the intersection point with the BLF regime, or the calculation of the BLF regime reaches the intersection point with the FLF regime. It is (1.5) when the calculation reaches the intersection point between formation and BDF regime.

6- Calculate the flow rate of the second flow regime using Eq. (24) with consideration given to the correction factor (β). Continue the flow rate calculations until the last flow rate of the second flow regime.

7- Repeat step-5 and 6 for the next flow regime until the production history is completed.

8- When the calculations have reached the last two flow rates and the corresponding production times in the production history, assume future production time and calculate the future flow rate corresponding to that time using Eq. (24).
9- Using the calculated flow rate in step-8, calculate the RNFD using Eq. (23).
10- Calculate the new flow rate corresponding to the new assumed production time and repeat step-9. Continue the calculations until reaching the abandonment flow rate.
11- Plot on the same log-log scale used for plotting the production history, the calculated flow rate vs. production time, and compare with the production history.
12- Plot the calculated RNFD and plot it on the same log-log plot of the actual RNFD, calculated using the production history, and compare the two. The excellent match between the two RNFDs indicates the accuracy of the simulated and predicted flow rates.
13- Calculate the cumulative production using the calculated flow rate during the production history and the future time using Eq. (26). Plot the cumulative production on a semi-log plot.

The impact of skin factor

Mathematically, the constant behavior of the RNFD of all flow regimes, shown in Eqs. (19), (20), (21), and (22) assumes the impact of skin factor does not exist. In reality, the production history may undergo this impact. Typically, this impact is seen in the calculated RNFD and flow rate by the proposed approach from the production history. Fig. (7) describes this impact on the normalized flow rate derivative. The following comments are inferred from Fig. (7):

1- The impact of the skin factor leads to a decrease in the flow rate that leads to a shift down the normalized flow rate curve, i.e., the RNFD curve. The constant behavior of the RNFD is no longer seen when the flow rate experiences the impact of the skin factor. Instead, the RNFD shows straight lines of a positive slope with time. The slopes of these lines depend on the severity of the skin factor impact.
2- The impact of the skin factor is seen very clearly during early production when the reservoir fluid flow is dominated by HFLF regime. It could continue beyond early production when the BLF regime has reached. If there is a severe impact, the FLF regime might be slightly affected also.
3- It is uncommon to see this impact during late production when the BDF regime is reached.
4- It is reasonably accepted to consider the impact of the skin factor on the hydraulic fracture and BLF regime only. Accordingly, it has been found that the slope of the fully developed straight line of the RNFD corresponds to the HFLF regime (0.5). The slope of the RNFD corresponds to the BLF regime (0.25) when there is a severe skin factor impact.
5- Suppose the production history shows either the FLF regime or the BDF regime as the last observed flow regime. In that case, the predicted flow rate by the proposed approach may not be affected significantly by the impact of the skin factor.

The impact of the skin factor can be included in the RNFD models of the hydraulic fracture and BLF regimes. Fig. (7) demonstrates a linear relationship between the RNFD with time when a severe skin factor controls the production history, especially at early time flow regimes. Accordingly, Eqs. (19) and (20) can be replaced by the following models:

$$\frac{1}{q}\left(txq^{'}\right) = -m_{hf} - C$$

(28)

$$\frac{1}{q}\left(txq^{'}\right) = -m_{blf} - C$$

(29)

Eqs. (28) and (29) suggest that the log-log plot of the actual RNFD calculated from the production history at early production time gives two straight lines. The slope of the first line corresponds to the HFLF regime is $\left(m_{hf}\right)$. The slope of the second line corresponds to the BLF regime is $\left(m_{blf}\right)$. The intersection points of these two lines with the RNFD axis give the intercept (C) for each flow regime.

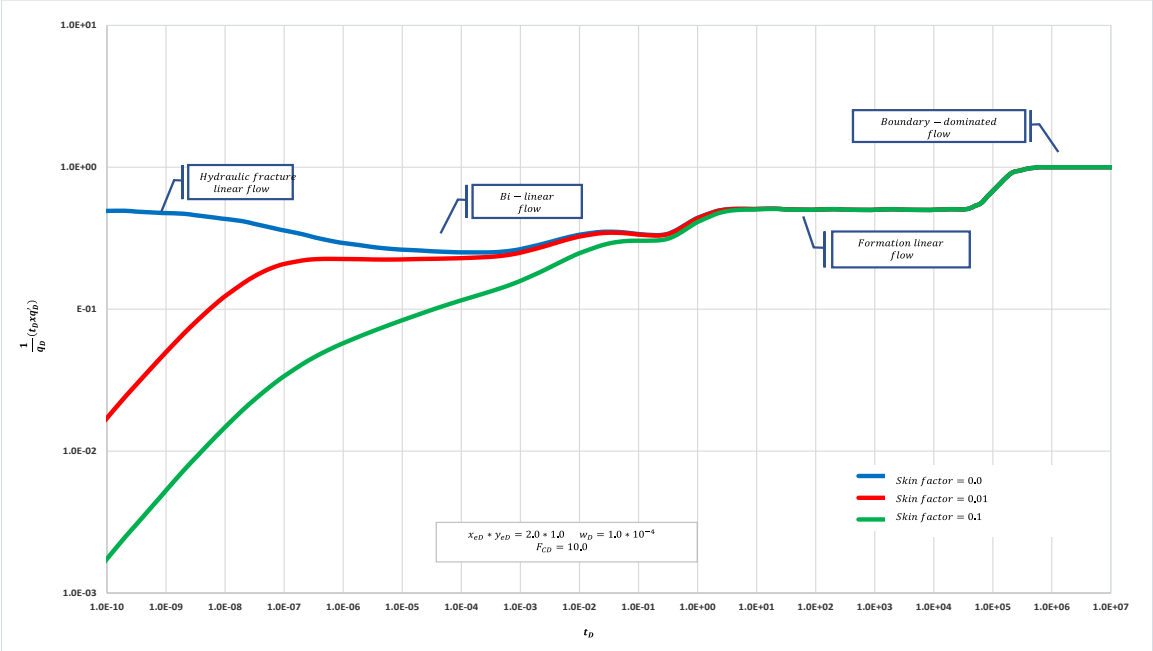

Figure 7: The impact of skin factor on the normalized flow rate derivative.

Case studies

The proposed RNFD decline curve technique has been exercised using the production history of four gas and oil-producing wells from different shale layers in the USA and Canada.

5-1- Case Study-1

A horizontal well is drilled in the Barnet Shale, TX, USA, and intersected by multiple hydraulic fractures (16 fractures and 4 fracturing stages). This well started production in 2006 and continued five years. The matrix permeability is close to 0.0025 md, and the fracture half-length is close to 150 ft. The drainage area is 33 acres, and the estimated initial gas in place is 3.2 BScf (Strickland and Blasingame 2011).

The production history has been digitalized to create a production time-flow rate table. The log-log plot of the flow rate vs. production time demonstrates two straight lines. The first shows a slope (0.5) while the second characterizes by a slope of (1.0). Accordingly, the first line represents the FLF regime, while the second is the BDF regime. Neither HFLF regime nor bilinear flow regime is observed. The end time of the BLF regime and the start time of the BDF regime is determined from the intersection point of the two flow regimes (300 days). The actual RNFD of the production history is calculated by Eq. (23) for real-time parameters. The computed RNFD data has been processed, smoothed, and plotted vs production time. It shows two horizontal lines; the first confirms the FLF regime as it appears with a constant value close to (0.5), while the second confirms the BDF regime with a constant value of (1.0).

Eq. (24) simulates the flow rate during the formation linear and BDF regimes. The simulated RNFD is calculated by Eq. (26) and plotted vs production time. The correction factor ($\beta = 1.5$) is used for the BDF regime. Accordingly, the future performance of the reservoir is forecasted using Eq. (24) based on the (RNFD=1.0) of the BDF regime and the correction factor ($\beta = 1.5$). The simulated and predicted flow rate, calculated by the RNFD, and the production history are plotted on the log-log scale as it is shown in Fig. (8a). While the simulated and predicted RNFD and the actual RNFD are plotted vs production time as it is shown in Fig. (8b). Figs. (8a) demonstrates an excellent matching with the production history, while matching the simulated RNFD and the actual RNFD, shown in Fig. (8b), is reasonable. The reason for that is the digitalization process of the production history that may not match precisely the production history as well as the data processing after the digitalization. Moreover, the production history already includes the impact of the skin factor and the wellbore conditions that could deteriorate the actual production, while RNFD does not consider either the reservoir or the wellbore conditions.

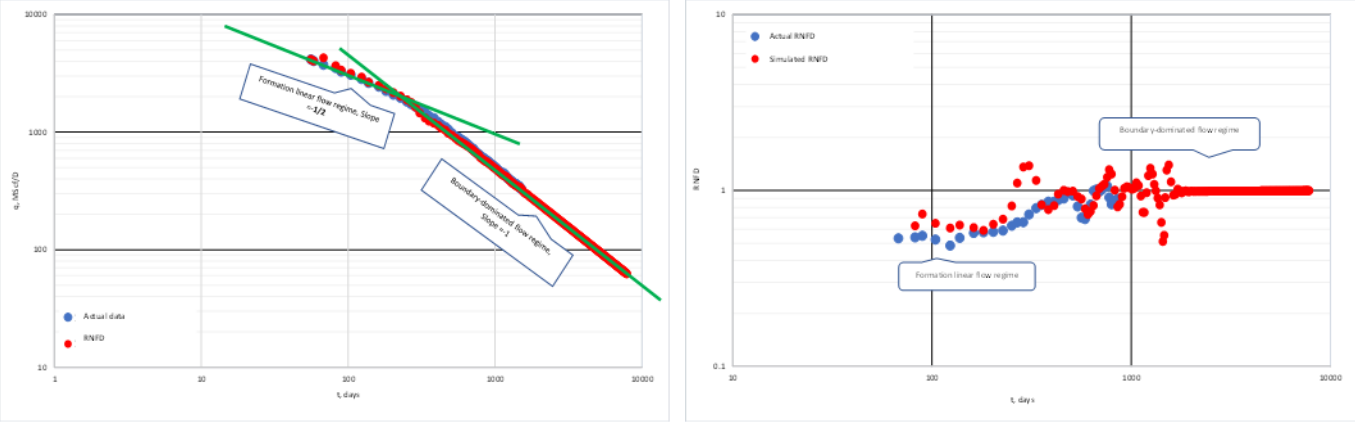

(a) (b)

Figure 8 :(a) Actual and simulated flow rate, calculated by RNFD, behaviors for Study-1, (b) Actual and simulated RNFD behaviors for Case- Study-1.

The simulated and predicted flow rates are compared with the production history, shown in the original paper presented by Strickland and Blasingame 2011. The comparison shows an excellent matching is it is seen in Fig. (9). The cumulative production is calculated and plotted in Fig. (10). The estimated ultimate recovery after 20 years is determined analytically

using Eq. (27) and graphically from Fig. (10). It is $\left(EUR|_{20years} = 2.35\ BScf\right)$. The EUR calculated by the Arps decline curve is 1.8 BScf considering that the exponential decline is (b=0.71) while the simulation software (Kappa Topaze) is 2.0 BScf (Strickland and Blasingame 2011).

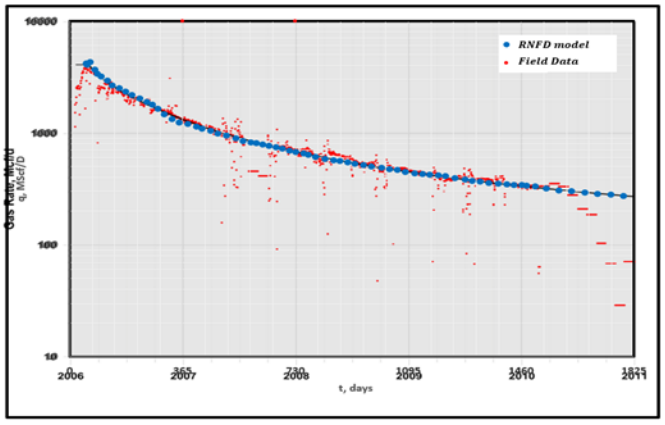

Figure 9:Comparison of the RNFD results and the production history for Case-Study-1.

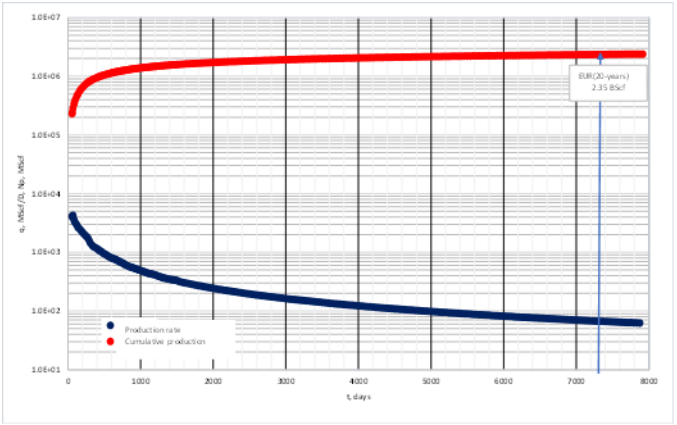

Figure 10: The flow rate and cumulative production of Case-Study-1.

Case Study-2

The production history of another Barnet Shale gas-producing well located in Denton County, TX, USA, is used in this study. The well has a lateral length of 8500 ft. The production from this well started in 2013 with more than 4-5 MMScf/D and continued to 2.5 MMScf/D after 3.5 years. The production history of this well is presented by Odi et al. 2019. The production history indicates two flow regimes; the first is the BLF regime represented by a straight line of a slope (0.25). The second is the FLF regime represented by a straight line of a slope (0.5). These two flow regimes are observed at the log-log plots of the flow rate and actual RNFD vs. production time. From the production history, the starting time of the BLF regime is determined to be (100 days) while the starting time of the FLF regime is determined to be (900 days). These two times are determined from the log-log plot of the field production data vs. production time.

The early production data may indicate a skin factor or the surface choking effect; therefore, the HFLF regime is not seen. The BDF regime is also not seen, probably because the production has not reached the reservoir boundary. The simulated and predicted flow rate and the simulated and predicted NRFD are plotted and compared with the production history as depicted in Fig. (11a,b). The correction factor $(\beta = 3.0)$ is used to calculate the flow rate during the FLF regime and predict future performance beyond this flow regime. The simulated and predicted flow rate behavior closely matches the results of Arps's traditional decline curve model with an exponential decline (b=4.0) calculated by Odi et al. 2019.

Similar to case study-1, Fig. (11a) shows an excellent matching between the actual flow rate data and the calculated flow rate by the RNFD except for very early production data $(t < 70\ days)$ wherein the impact of the wellbore conditions and the skin factor may deteriorate the production. However, the calculated flow rates by the RNFD for the early production data are close to demonstrating the HFLF regime where the slope of the log-log plot of production rate vs production time is (0.5).

Therefore, the difference between the calculated flow rate by the RNFD and the actual flow rate taken from the production history indicates the severity of the skin factor at early production time. The actual and simulated RNFD behaviors, shown in Fig. (11b), demonstrate a very close match.

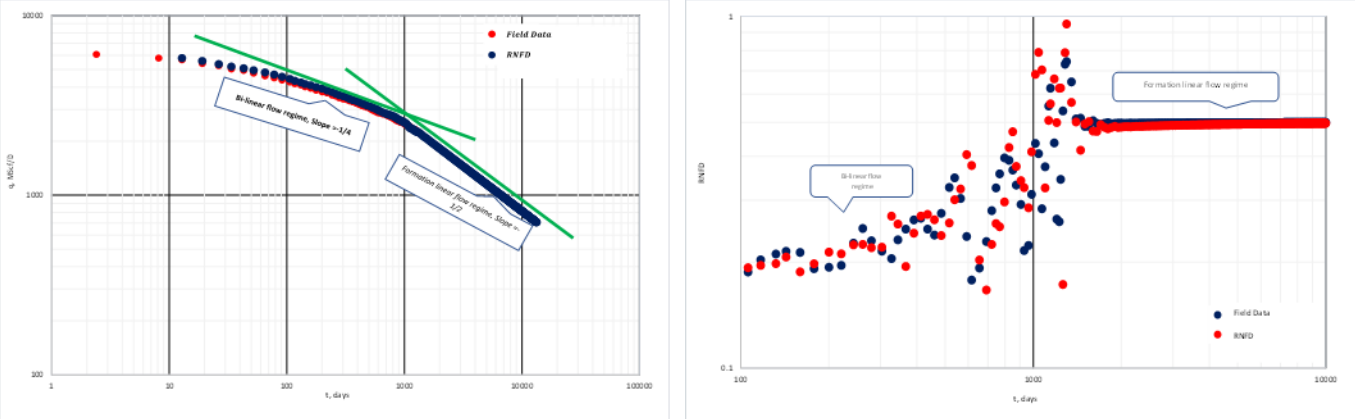

(a) (b)

Figure11 : (a) Actual and simulated flow rate, calculated by RNFD, behaviors for Study-2, (b) Actual and simulated RNFD behaviors for Case- Study-2.

The calculated flow rate has been plotted and compared with the production history, as shown in Fig. (12). An excellent matching is obtained. The flow rate and the cumulative production are plotted in Fig. (13), where the estimated ultimate recovery is $\left(EUR|_{20years} = 11.95\ BScf\right)$. The cumulative production calculated at the end of the production history is $(4.0\ BScf)$.

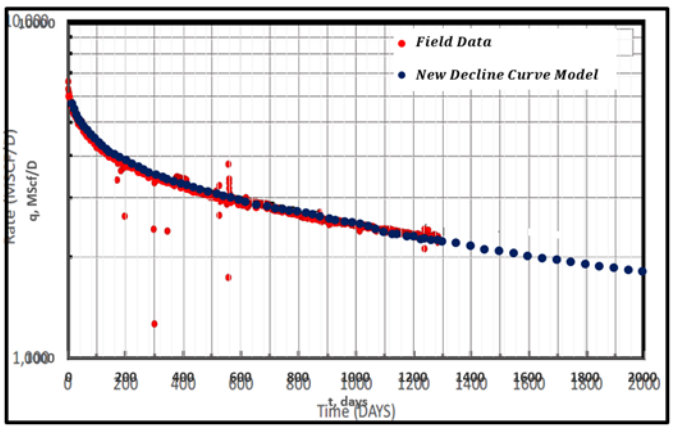

Figure 12: Comparison of the RNFD results and the production history for Case-Study-2.

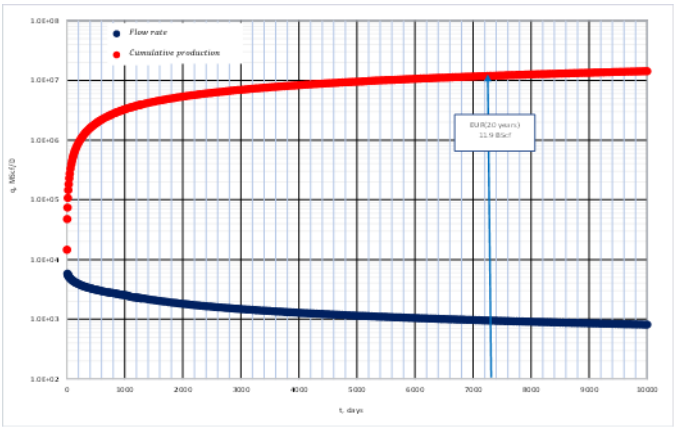

Figure 13: The flow rate and cumulative production of Case-Study-2.

Case Study-3

The production history of an oil-producing well from the Bakken Formation (Well UT-ID-220) is used in this case study (Hong et al. 2019). The well is completed with multiple hydraulic fractures. The production history includes the production

and the corresponding flow rate for almost two years (700 days). Bi-linear and FLF regimes are characterized from the production history. The starting time of the FLF regime is determined from the production history to be (180 days). The RNFD is used for simulating and predicting future performance. The correction factor ($\beta = 1.5$) is used for the FLF regime. The calculated flow rate and RNFD behaviors display an excellent match with the production history, as shown in Figs. (14a,b), and (15). The simulated and predicted behaviors of the production rate match exactly the flow rate behavior obtained by applying the combined probabilistic distribution (P_{mean}), as seen in Fig. (15). The cumulative production is plotted in Fig. (16). The estimated ultimate recovery is determined to be $\left(EUR|_{20years} = 157{,}400\ Stb\right)$.

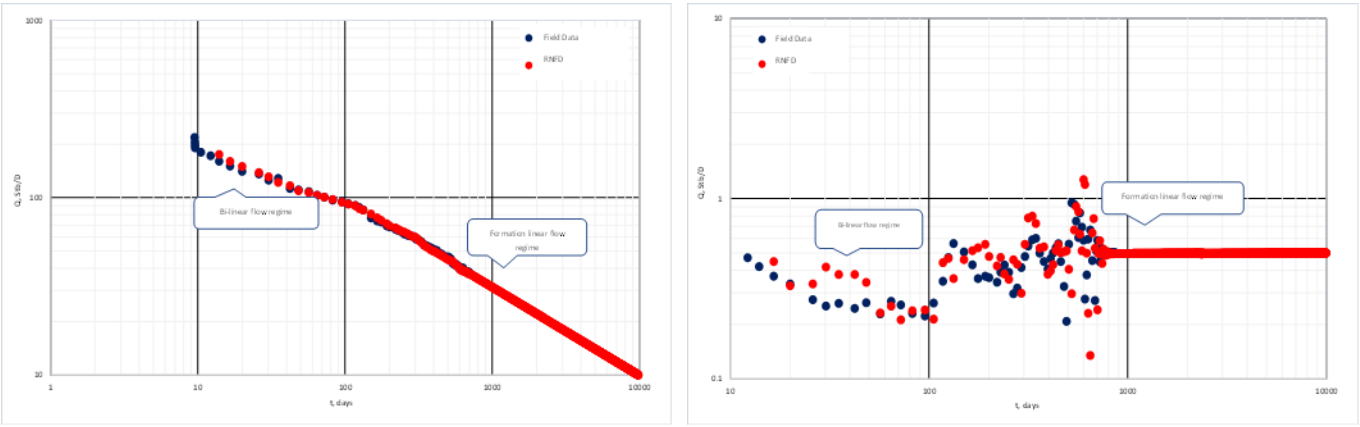

(a) (b)

Figure 14: (a) Actual and simulated flow rate, calculated by RNFD, behaviors for Study-3, (b) Actual and simulated RNFD behaviors for Case- Study-3

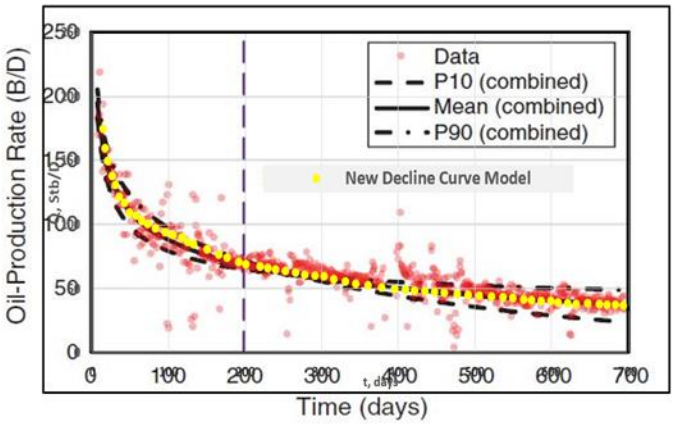

Figure 15: Comparison of the RNFD results and the production history for Case-Study-3.

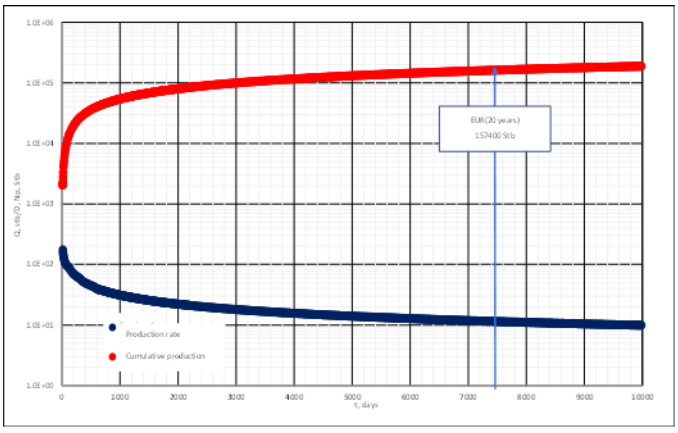

Figure 16: The flow rate and cumulative production of Case-Study-3.

Case Study-4

The production history of more than seven years of a dry gas-producing well in the Western Canada Sedimentary Basin (WCSB) is used in this case. This well is completed as an open hole with multiple hydraulic fractures (Yu et al. 2013; Shahamat et al. 2015). The production history is taken from the paper presented by Shahamat et al. 2015. The forecasting of future performance using the proposed RNFD technique and the comparison with the currently used DCA techniques are conducted in this case study. Two flow regimes are characterized from the production history, as shown in Fig. (17a). The first is the FLF regime, while the second is the BDF regime. The plot of the RNFD shown in Fig. (17b) confirms this observation. The correction factor ($\beta = 1.5$) is used for the calculations of the BDF regime.

The results of the proposed RNFD decline curve analysis are compared with the currently used DCA techniques, such as traditional Arps' decline curve models for the exponential decline (b=2.0) for the transient flow, and (b=0.5) for the BDF, stretched exponential, Duong model, and the Beta-Derivative method as shown in Fig. (18). The compassion shows that the RNFD gives flow rates higher than the Arps' decline curve models when the exponential decline of the BDF is used (b=0.5), stretched exponential, and the Beta-Derivative, but less than the flow rates calculated by Duong model and Arps' decline curve models when the exponential decline of the BDF is used (b=1.0). The cumulative production calculated by the RNFD is depicted in Fig. (19), wherein the estimated ultimate recovery is $\left(EUR|_{20years} = 2189.9\ MMScf\right)$. Table-1shows the EUR calculated by the proposed RNFD technique and the currently used DCA techniques. It is important to emphasize that the estimated ultimate recovery calculated by the proposed approach in this study is greater than the one calculated by the other techniques. The proposed approach considers the different flow regimes observed from the production history when calculating the flow rate.

Table 1: Comparison of the EUR

Technique	$EUR\|_{20years}, MMScf$
RNFD	2189.9
Beta-Derivative	1766
Arps	1919 for b=0.5 (boundary-dominated flow) 2408 for b=1.0 (boundary-dominated flow)
Stretched exponential	1914

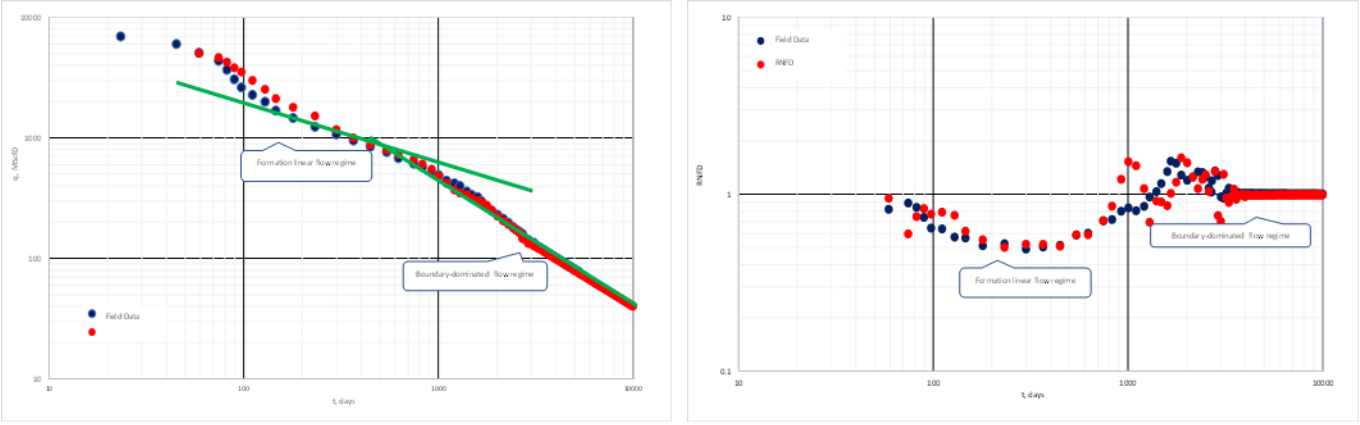

(a) (b)

Figure 17: (a) Actual and simulated flow rate, calculated by RNFD, behaviors for Study-4, (b) Actual and simulated RNFD behaviors for Case- Study-4

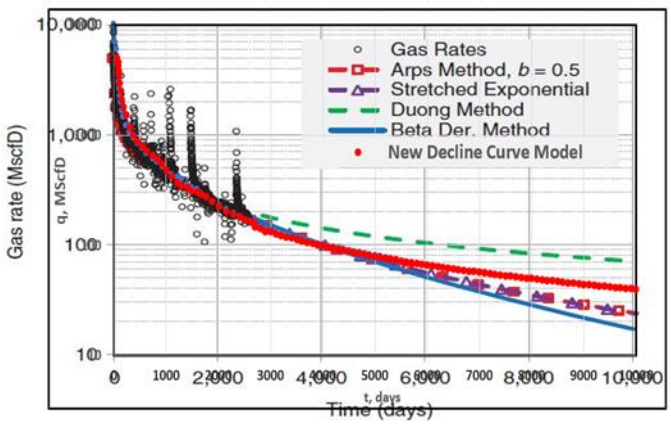

Figure 18: Comparison of the RNFD and the currently used decline curve analysis techniques for Case-Study-4.

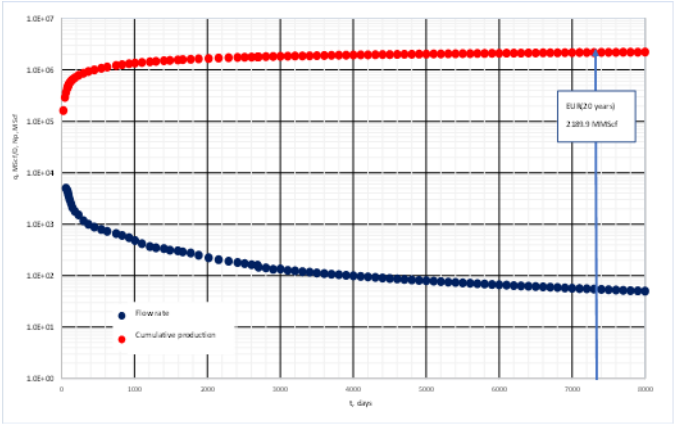

Figure 19: The flow rate and cumulative production of Case-Study-4.

Limitations

The proposed approach in this study can be applied confidently for forecasting future performance if the last observed flow regime from the production history is the BDF regime. The characteristic RNFD of this flow regime is (1.0). Sometimes the last observed flow regime may not be the BDF regime. Instead, the formation linear or BLF regime could be the last seen flow regime. Both are characterized by a constant RNFD of (0.5) and (0.25), respectively. Therefore, the predicted flow rates calculated based on the RNFD of one of them, the last seen, will be greater than those calculated based on the RNFD of the BDF regime. Fig. (20) depicts the predicted flow rate of the case study-2 wherein the FLF regime is the last observed flow regime. The blue dots represent the flow rates calculated based on the RNFD of the FLF regime and extended to 8000 production days. The red dots represent the flow rates assuming the BDF regime will be observed after 5000 production days. The RNFD of the BDF regime is used to predict the flow rates beyond 5000 production days and extended to 8000

production days. It has been found that the difference in the expected flow rates of the two cases is not significant. The flow rates calculated based on the FLF regime are greater than the BDF regime, but the difference is no more than (1.0%). Moreover, the estimated ultimate recovery (EUR) does not show a significant difference between the two cases. It drops to $\left(EUR|_{20years} = 11.3\ BScf\right)$ for the case of the BDF regime compared to $\left(EUR|_{20years} = 11.95\ BScf\right)$ for the FLF regime. Physically, when the BDF regime has reached, the reservoir pressure at the boundary decreases, thereby decreasing the sandface flow.

The difference in the predicted flow rates could be more significant if the BLF regime is the last observed flow regime. The RNFD of the BLF regime is (0.25); therefore, the calculated flow rate base on that is greater than the flow rate calculated based on the RNFD of the BDF regime (1.0). Consequently, it is recommended to determine the times when the FLF and BDF regimes are expected to be observed.

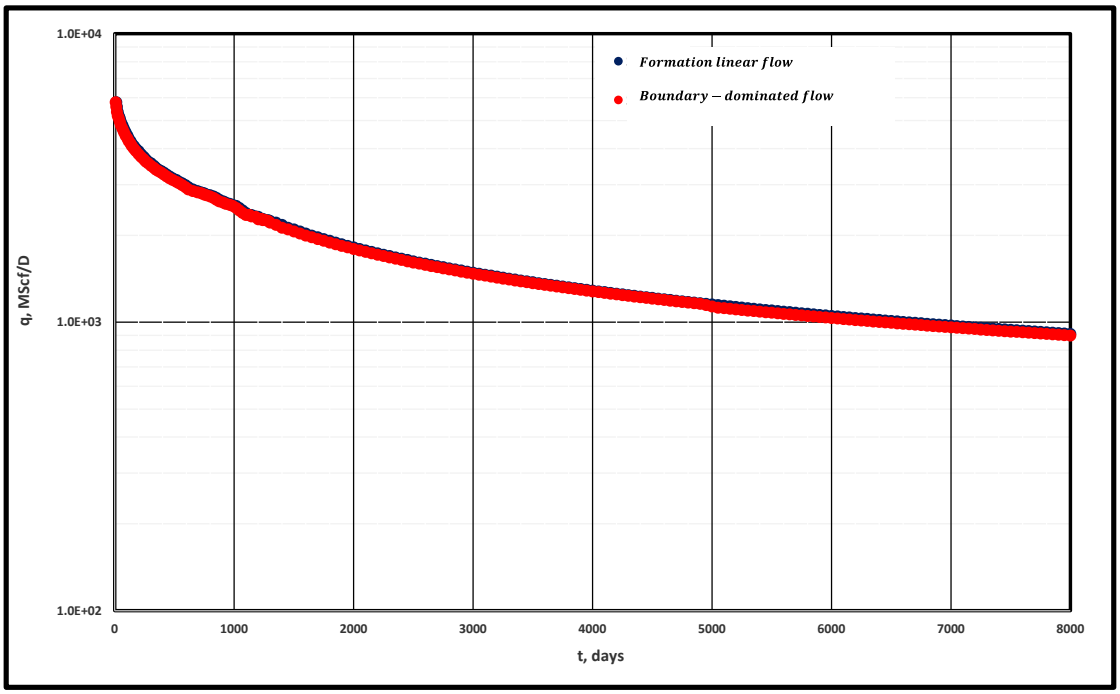

Figure 20: The difference in the predicted flow rates based on the FLF regime and the boundary-dominated flow regime.

Conclusions

The study has reached several conclusions:

1- The proposed approach in this study is an excellent tool for quickly and confidently forecasting the future performance of oil and gas-producing wells from unconventional reservoirs completed with multiple hydraulic fractures. It considers only the production history of the producing wells and does not consider the reservoir and wellbore conditions.

2- The RNFD behavior demonstrates a constant value for each flow regime with time. It has a value of (0.5) for hydraulic fracture and FLF regime, while it is (0.25) for the BLF regime and (1.0) for the BDF regime. However, the constant

pattern of the RNFD is no longer seen when the production history has experienced the impact of skin factor, especially at early production time flow regimes such as HFLF and BLF regimes.

3- The predicted flow rate by the proposed approach may not be affected significantly by the impact of skin factor if the last observed flow regime, from the production history, is either the FLF regime or the BDF regime. The effect of the skin factor and wellbore conditions may appear specifically at early production time when the production history has undergone this impact. Therefore, the predicted late production time flow rate matches the production history better than the earlier production time when hydraulic and BLF regimes dominate the flow.

4- The production history data is required to be processed and smoothed for better forecasting by the RNFD; however, the raw data of the production history can also be used by the proposed RNFD technique.

5- A correction factor (β) is required for the application of the RNFD. It is used to correct the change in the slope of the flow regimes when the calculations have reached the intersection point between these flow regimes, i.e., the starting of a new flow regime. The correction factor is (3.0) for the BLF that follows HFLF or FLF that follows the BLF, while it is (1.5) for the BDF regime.

6- The proposed approach in this study can be applied confidently for forecasting future performance if the last observed flow regime is the BDF regime. However, if this flow regime is not the last seen flow regime, the predicted flow rate could be slightly greater than the flow rate calculated by the RNFD of the BDF regime.

Abbreviations:

BDF	Boundary-dominated flow
BLF	Bi-linear flow
DCA	Decline curve analysis
EUR	Estimated ultimate recovery
FLF	Formation linear flow
HFLF	Hydraulic fracture linear flow
LGM	Logistic growth model
RNFD	Rate-normalized flow rate derivative
SRV	Stimulated reservoir volume
USRV	Un-stimulated reservoir volume

Nomenclatures:

c_t	Total compressibility, psi^{-1}
h	Formation thickness, ft
k	Permeability, md
N_P	Cumulative oil or gas production
N_{PD}	Cumulative oil or gas production, dimensionless
P_{wD}	Wellbore pressure drop, dimensionless
ΔP	Wellbore pressure drop, psi
q	Surface flow rate, Scf/D
$q^{'}$	Surface flow rate derivative, (Scf/D)/D
q_D	Surface flow rate, dimensionless
$q_D^{'}$	Surface flow rate derivative, dimensionless

s	Laplace operator
t	Production time, hrs
t_D	Production time, dimensionless
τ_D	Dummy variable of time
T	Temperature, R
x_{eD}	Reservoir boundary, dimensionless
x_e	Reservoir boundary, ft
x	Any point in the X-direction
x_f	Hydraulic fracture half-length, ft
y_{eD}	Reservoir boundary, dimensionless
y_e	Reservoir boundary, ft
y	Any point in the Y-direction
w_D	Hydraulic fracture width, dimensionless
w_f	Hydraulic fracture width, ft
μ	Viscosity, cp
$\emptyset$	Porosity, fraction
η	Hydraulic diffusivity

Subscript

f	Hydraulic fracture
srv	Stimulated reservoir volume
$usrv$	Unstimulated reservoir volume
i	Current time step
$i+1$	The time step after the current
$i-1$	The time step before the current

References:

[1] Alarifi, Sulaiman A., and Jennifer Miskimins, 2021. A New Approach to Estimating Ultimate Recovery for Multistage Hydraulically Fractured Horizontal Wells by Utilizing Completion Parameters Using Machine Learning. SPE Production and operation, 36(03).

[2] Al-Rbeawi, S., 2018. Bivariate Log-Normal Distribution of Stimulated Matrix Permeability and Block Size in Fractured Reservoirs: Proposing New Multilinear-Flow Regime for Transient-State Production. SPE Journal, 23 (04), pp.1316-1342.

[3] Al-Rbeawi, S., 2020. The impact of spatial and temporal variability of anomalous diffusion flow mechanisms on reservoir performance in structurally complex porous media. Journal of Natural Gas Science and Engineering, 78(2020), 103331.

[4] Arps, J.J. 1945. Analysis of Decline Curves. Petroleum Development and Technology 160 (1): 228–247. SPE-945228-G. New York: Transactions of the American Institute of Mining and Metallurgical Engineers, AIME.

[5] Ayala, Luis, and Miao Zhang, 2013. Rescaled Exponential and Density-Based Decline Models: Extension to Variable Rate/Pressure-Drawdown Conditions. Journal of Canadian Petroleum Technology 52 (06): 433–440.

[6] Bello, Rasheed O., and Robert A. Wattenbarger, 2010. Multistage Hydraulically Fractured Shale Gas Rate Transient Analysis. Paper presented at the North Africa Technical Conference and Exhibition, Cairo, Egypt.

[7] Blasingame, T.A., and W.J. Lee, 1986. Variable-Rate Reservoir Limits Testing. Paper presented at the Permian Basin Oil and Gas Recovery Conference, Midland, Texas.

[8] Blasingame, and Jay Alan Rushing, 2005. A Production-Based Method for Direct Estimation of Gas in Place and Reserves. Paper presented at the SPE Eastern Regional Meeting, Morgantown, West Virginia.

[9] Brown, M., Ozkan, E., Raghavan, R., & Kazemi, H., 2011. Practical Solutions for Pressure-Transient Responses of Fractured Horizontal Wells in Unconventional Shale Reservoirs. SPE Reservoir evaluation & engineering, 14(6), pp. 663-676.

[10] Can, B.., and C.S. S. Kabir, 2011. Probabilistic Production Forecasting for Unconventional Reservoirs with Stretched Exponential Production Decline Model. SPE Reservoir Eval & Engineering 15 (01): 41–50.

[11] Chavali, V. B. K., and W. J. Lee, 2021. Fast Probabilistic Forecasting of Oil Production using Monte Carlo Simulations on Data Driven Acquisition of Decline-Curve Parameter Distributions. Paper presented at the SPE/AAPG/SEG Unconventional Resources Technology Conference, Houston, Texas, USA.

[12] Clark, A. J., Lake, L. W., and T. W. Patzek, 2011. Production Forecasting with Logistic Growth Models. Paper presented at the SPE Annual Technical Conference and Exhibition, Denver, Colorado, USA.

[13] de Holanda, Rafael Wanderley, Gildin, Eduardo, and Peter P. Valkó., 2018. Combining Physics, Statistics, and Heuristics in the Decline-Curve Analysis of Large Data Sets In Unconventional Reservoirs. SPE Reservoir Evaluation & Engineering 21 (03): 683–702.

[14] Duong, Anh N., 2011. Rate-Decline Analysis for Fracture-Dominated Shale Reservoirs. SPE Reservoir Evaluation & Engineering 14 (03): 377–387.

[15] Egbe, U. C., Awoleke, O. O., Olorode, O. M., and S. D. Goddard, 2023. On the Application of Probabilistic Decline Curve Analysis to Unconventional Reservoirs. SPE Reservoir Evaluation & Engineering, 26(02): 244–260.

[16] El-Banbi, Ahmed H., and Robert A. Wattenbarger, 1998. Analysis of Linear Flow in Gas Well Production. Paper presented at the SPE Gas Technology Symposium, Calgary, Alberta, Canada.

[17] Fetkovich, M.J. 1980. Decline Curve Analysis Using Type Curves. Journal of Petroleum Technology 32 (6): 1065–1077. SPE-4629-PA.

[18] Fetkovich, M.J., Fetkovich, E.J., and Fetkovich, M.D. 1996. Useful Concepts for Decline Curve Forecasting, Reserve Estimation, and Analysis. SPE Reservoir Evaluation & Engineering 11 (1): 13–22. SPE-28628-PA.

[19] Fetkovich, M.J., Vienot, M.E., Bradley, M.D. et al. 1987. Decline Curve Analysis Using Type Curves: Case Histories. SPE Formation Evaluation 2 (4): 637–656. SPE-13169-PA.

[20] Fraim, M. L., and R. A. Wattenbarger, 1987. Gas Reservoir Decline-Curve Analysis Using Type Curves with Real Gas Pseudopressure and Normalized Time. SPE Formation Evaluation 2 (04): 671–682.

[21] Fulford, David S., Bowie, Braden, Berry, Michael E., Bowen, Bo, and Derrick W. Turk, 2016. Machine Learning as a Reliable Technology for Evaluating Time/Rate Performance of Unconventional Wells. SPE Economic and management, 8 (01).

[22] Gupta, Ishank, Rai, Chandra, Sondergeld, Carl, and Deepak Devegowda, 2018. Variable Exponential Decline: Modified Arps To Characterize Unconventional-Shale Production Performance. SPE Reservoir Evaluation & Engineering 21 (04): 1045–1057.

[23] Hazlett, R. D., Farooq, U., and D. K. Babu, 2021. A Complement to Decline Curve Analysis. SPE Journal 26 (04): 2468–2478.

[24] He, Si, Ge, Hongkui, Zhang, Jialiang, Shen, Yinghao, and Xiaoqiong Wang, 2022. Application of Decline Analysis in Shale Oil Productivity Evaluation and Prediction: A Case Study of Jimsar Shale Oil. Paper presented at the 56th U.S. Rock Mechanics/Geomechanics Symposium, Santa Fe, New Mexico, USA.

[25] Helmy, M. W., & Wattenbarger, R. A.,1998. New Shape Factors for Wells Produced at Constant Pressure. Paper presented at the SPE gas technology symposium held in Calgary, Canada.

[26] Hong, Aojie, Bratvold, Reidar B., Lake, Larry W., and Leopoldo M. Ruiz Maraggi, 2019. Integrating Model Uncertainty in Probabilistic Decline-Curve Analysis for Unconventional-Oil-Production Forecasting. SPE Reservoir Evaluation & Engineering, 22 (2019): 861–876.

[27] Hsieh, Frank S., Vega, Cecilia, and Lucy Vega, 2001. Applying a Time-Dependent Darcy Equation for Decline Analysis for Wells of Varying Reservoir Type. Paper presented at the SPE Rocky Mountain Petroleum Technology Conference, Keystone, Colorado.

[28] Idorenyin, E., Okouma, V., and L. Mattar, 2011. Analysis of Production Data Using the Beta-Derivative. Paper presented at the Canadian Unconventional Resources Conference, Calgary, Alberta, Canada.

[29] Ilk, D., Currie, S. M., and T. A. Blasingame, 2010. Production Analysis and Well Performance Forecasting of Tight Gas and Shale Gas Wells. Paper presented at the SPE Eastern Regional Meeting, Morgantown, West Virginia, USA.

[30] Ilk, D., Rushing, J. A., and T. A. Blasingame, 2011. Integration of Production Analysis and Rate-Time Analysis via Parametric Correlations — Theoretical Considerations and Practical Applications. Paper presented at the SPE Hydraulic Fracturing Technology Conference, The Woodlands, Texas, USA.

[31] Ilk, D., Hosseinpour-Zonoozi, N., Amini, S., and T. A. Blasingame, 2007.Application of the β-Integral Derivative Function to Production Analysis. Paper presented at the Rocky Mountain Oil & Gas Technology Symposium, Denver, Colorado, U.S.A.

[32] Johnson, R.H. and Bollens, A.L., 1927. The Loss Ratio Method of Extrapolating Oil Well Decline Curves. Trans. of the AIME 77 (1): 771–778. SPE-927771-G.

[33] Kuchuk, F., Morton, K., & Biryukov, D., 2016. Rate-Transient Analysis for Multistage Fractured Horizontal Wells in Conventional and Un-Conventional Homogeneous and Naturally Fractured Reservoirs. Paper presented at the SPE annual Technical Conference & Exhibition held in Dubai, UAE.

[34] Lee, John, and Rod Sidle, 2010. Gas-Reserves Estimation in Resource Plays. SPE Economics & Management 2 (02): 86–91.

[35] Liu, Shuai, and Peter P. Valkó, 2019. Production-Decline Models Using Anomalous Diffusion Stemming From a Complex Fracture Network. SPE J0urnal 24 (06): 2609–2634.

[36] Liu, Hui-Hai, Zhang, Jilin, Liang, Feng, Temizel, Cenk, Basri, Mustafa A., and Rabah Mesdour, 2021. Incorporation of Physics into Machine Learning for Production Prediction from Unconventional Reservoirs: A Brief Review of the Gray-Box Approach. SPE Reservoir Evaluation & Engineering 24 (04): 847–858.

[37] Liu, Zizhong, and Hamid Emami-Meybodi, 2021. Diffusion-Based Modeling of Gas Transport in Organic-Rich Ultratight Reservoirs. SPE Journal, 26 (2021): 857–882.

[38] Luo, H.., Mahiya, G.F. F., Pannett, S., and P. Benham, 2014. The Use of Rate-Transient-Analysis Modeling to Quantify Uncertainties in Commingled Tight Gas Production-Forecasting and Decline-Analysis Parameters in the Alberta Deep Basin. SPE Reservoir Evaluation & Engineering 17 (02): 209–219.

[39] Maraggi, Leopoldo M. Ruiz, Walsh, Mark P., and Larry W. Lake, 2023. A New Approach to Apply Decline-Curve Analysis for Tight-Oil Reservoirs Producing Under Variable Pressure Conditions. Paper presented at the SPE/AAPG/SEG Unconventional Resources Technology Conference, Denver, Colorado, USA.

[40] Mattar, L., Gault, B., Morad, K., Clarkson, C. R., Freeman, C. M., Ilk, D., and T. A. Blasingame, 2008. Production Analysis and Forecasting of Shale Gas Reservoirs: Case History-Based Approach. Paper presented at the SPE Shale Gas Production Conference, Fort Worth, Texas, USA.

[41] Minin, Antonio, Guerra, Laura, and Ivan Colombo, 2011. Unconventional Reservoirs Probabilistic Reserve Estimation Using Decline Curves. Paper presented at the International Petroleum Technology Conference, Bangkok, Thailand.

[42] Odi, Uchenna, Bacho, Sarah, and Johan Daal, 2019. Decline Curve Analysis in Unconventional Reservoirs Using a Variable Power Law Model: A Barnett Shale Example. Paper presented at the SPE/AAPG/SEG Unconventional Resources Technology Conference, Denver, Colorado, USA.

[43] Ozkan, O., Sarak, H., Ozkan, E., and Raghavan, R., 2014: A trilinear flow model for a fractured horizontal well in a fractal unconventional reservoir. Paper presented at the SPE annual technical conference and exhibition held in Amsterdam, Netherland.

[44] Raghavan, R., Chen, C., 2017. Rate decline, power laws, and subdiffusion in fractured rocks. SPE Reservoir Evaluation and Engineering, 20 (3), 738–751..

[45] Shahamat, M.S. S., Mattar, L., and R. Aguilera, 2015. Analysis of Decline Curves on the Basis of Beta-Derivative. SPE Reservoir Evaluation & Engineering 18 (2015): 214–227.

[46] Strickland, R., Purvis, D., and T. Blasingame, 2011. Practical Aspects of Reserve Determinations for Shale Gas. Paper presented at the North American Unconventional Gas Conference and Exhibition, The Woodlands, Texas, USA.

[47] Stright, D.H., and J.I. Gordon, 1983. Decline Curve Analysis in Fractured Low Permeability Gas Wells in the Piceance Basin. Paper presented at the SPE/DOE Low Permeability Gas Reservoirs Symposium, Denver, Colorado.

[48] Sureshjani, M. Heidari, and Shahab Gerami, 2011. A New Model for Modern Production-Decline Analysis of Gas/Condensate Reservoirs. Journal of Canadian Petroleum Technology 50 (07): 14–23.

[49] Valkó, Peter P, 2009. Assigning value to stimulation in the Barnett Shale: a simultaneous analysis of 7000 plus production hystories and well completion records. Paper presented at the SPE Hydraulic Fracturing Technology Conference, The Woodlands, Texas.

[50] Valkó, Peter P., and W. John Lee, 2010. A Better Way to Forecast Production from Unconventional Gas Wells. Paper presented at the SPE Annual Technical Conference and Exhibition, Florence, Italy.

[51] Van Everdingen, A.F., 1949. The application of the Laplace transformation to flow problems in reservoirs. Petroleum Transaction, AIME, 186, pp.305-324.

[52] van Kruysdijk, C.P.J.W. and Dullaert, G.M., 1989. A Boundary Element Solution of the Transient Pressure Response of Multiply Fractured Horizontal Wells. Paper presented at the 2nd European Conference on the Mathematics of Oil Recovery, Cambridge, England.

[53] Wang, HanYi, 2016. What Factors Control Shale-Gas Production and Production-Decline Trend in Fractured Systems: A Comprehensive Analysis and Investigation. SPE Journal 22 (02): 562–581.

[54] Wattenbarger, Robert A., El-Banbi, Ahmed H., Villegas, Mauricio E., and J. Bryan Maggard, 1998. Production Analysis of Linear Flow into Fractured Tight Gas Wells. Paper presented at the SPE Rocky Mountain Regional/Low-Permeability Reservoirs Symposium, Denver, Colorado.

[55] Xi, Zhenke, and Eugene Morgan, 2019. Combining Decline-Curve Analysis and Geostatistics To Forecast Gas Production in the Marcellus Shale. SPE Reservoir Evaluation & Engineering 22 (04): 1562–1574.

[56] Yu, Shaoyong, Lee, W. John, Miocevic, Dominic J., Li, Dong, and Seth Harris, 2013. Estimating Proved Reserves in Tight/Shale Wells Using the Modified SEPD Method. Paper presented at the SPE Annual Technical Conference and Exhibition, New Orleans, Louisiana, USA.

Appendix-A: Dimensionless parameters.

$$P_D = \frac{k_{srv} h \Delta P}{1422 q T} \quad \text{(A-1)}$$

$$t_D = \frac{0.000263 k_{srv} t}{(\emptyset \mu c_t)_{srv} x_f^2} \quad \text{(A-2)}$$

$$q_D = \frac{1422 q T}{k_{srv} h \Delta P} \quad \text{(A-3)}$$

$$N_{PD} = \frac{1422 T \int_0^t q d\tau}{k_{srv} h \Delta P} \quad \text{(A-4)}$$

$$x_D = \frac{x}{x_f} \quad \text{(A-5)}$$

$$y_D = \frac{y}{x_f} \quad \text{(A-6)}$$

$$w_D = \frac{w_f}{x_f} \quad \text{(A-7)}$$

$$x_{eD} = \frac{x_e}{x_f} \quad \text{(A-8)}$$

$$y_{eD} = \frac{y_e}{x_f} \quad \text{(A-9)}$$

$$R_{CD} = \frac{k_{srv} x_f}{k_{usrv} y_e} \quad \text{(A-10)}$$

$$\eta_{rD} = \frac{\eta_{usrv}}{\eta_{srv}} \quad \text{(A-11)}$$

$$\eta_{fD} = \frac{\eta_f}{\eta_{srv}} \quad \text{(A-12)}$$

$$\eta_f = \frac{(k/\mu)_f}{(\phi c_t)_f} \quad \text{(A-13)}$$

$$\eta_{srv} = \frac{(k/\mu)_{srv}}{(\phi c_t)_{srv}} \quad \text{(A-14)}$$

$$\eta_{usrv} = \frac{(k/\mu)_{usrv}}{(\phi c_t)_{usrv}} \quad \text{(A-15)}$$